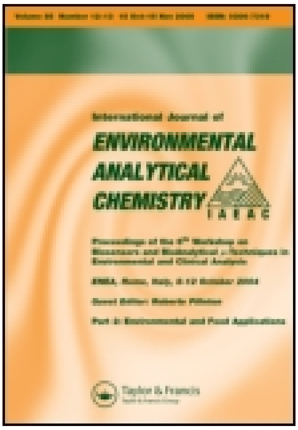

International Journal of Environmental Analytical Chemistry
Publication details, including instructions for authors and subscription information:
http://www.tandfonline.com/loi/geac20

Traceability study of hay with a mass spectrometer based on ion-molecule reactions of krypton, xenon and mercury using multivariate data analysis

Simon M. Valtiner [a], Christian Bachmann [b] & Christian W. Huck [a]
[a] Institute of Analytical Chemistry and Radiochemistry, Leopold-Franzens University, Innsbruck, Austria
[b] Agency for Environment of the Autonomous Province of Bozen-Südtirol, Bozen, Italy

To cite this article: Simon M. Valtiner, Christian Bachmann & Christian W. Huck (2012): Traceability study of hay with a mass spectrometer based on ion-molecule reactions of krypton, xenon and mercury using multivariate data analysis, International Journal of Environmental Analytical Chemistry, 92:2, 237-254

To link to this article: http://dx.doi.org/10.1080/03067319.2010.548603

Intern. J. Environ. Anal. Chem.
Vol. 92, No. 2, 15 February 2012, 237–254

Taylor & Francis
Taylor & Francis Group

Traceability study of hay with a mass spectrometer based on ion-molecule reactions of krypton, xenon and mercury using multivariate data analysis

Simon M. Valtiner[a], Christian Bachmann[b] and Christian W. Huck[a]*†

[a]*Institute of Analytical Chemistry and Radiochemistry, Leopold-Franzens University, Innsbruck, Austria;* [b]*Agency for Environment of the Autonomous Province of Bozen-Südtirol, Bozen, Italy*

(*Received 11 August 2010; final version received 2 December 2010*)

The application of mountain hay for wellness purposes has led to a substantial valorisation. To assure the quality associated with the high standards of production, which are often related to a characteristic distribution of plants and a variety of essential oils, a mass spectrometer, based on ion-molecule-reactions (IMR) of mercury, krypton and xenon, was employed to analyse characteristic VOCs of hay such as coumarin or typical monoterpenes and then used to develop an approach for the traceability of single hay samples based on concepts of multivariate statistics. The application of the primary gases to aqueous solutions of the pure compounds shows their suitability to deal with this problem, reveals important factors for the creation of a measurement set-up of such gas mixtures and indicates different mechanisms for the fragmentation, as shown for coumarin. The limit of determination ($3*s_R/SEN$) for aqueous solutions of p-cymene is $0.13\,mg\,L^{-1}$ using PLS1 and the presented combined mercury and xenon set-up, which confirms that this strategy is appropriate for an integration of compounds, which are present in low concentrations only, into a qualitative model. The results of the principal component analyses (PCA) of 136 hay samples were verified for the suitability to characterize single types of hay using three measurements of nine mountain hay samples, three normal hay samples and three aftermath samples for evaluation and applying SIMCA for classification at a significance level of 5%. The traceability of mountain hay samples is good (93% correctly classified) and can be used to protect these valuable samples.

Keywords: coumarin; hay; ion-molecule-reaction; multivariate data analysis; phytochemical analysis; terpenes; traceability

1. Introduction

In times of globalisation new innovative marketing strategies are of supreme importance. Especially in the field of agricultural products these include the highlighting of a product's origin and the emphasis of the production site as a distinctive cachet [1].

This work refers to the application of hay for wellness purposes like hay baths, a traditional [2,3] wellness offer in the Alpine regions. Since the plant combination of hay [4]

---

*Corresponding author. Email: Christian.W.Huck@uibk.ac.at

†Permanent address: Leopold-Franzens University Innsbruck, Institute of Analytical Chemistry and Radiochemistry, Innrain 52a, A-6020 Innsbruck, Austria.

ISSN 0306–7319 print/ISSN 1029–0397 online

http://dx.doi.org/10.1080/03067319.2010.548603
http://www.tandfonline.com

and hence the composition of essential oils, which are typical for the hay's odour, can vary considerably from one region [5] to another, the attributed therapeutic effects [6–8] should diverge to the same degree. This aspect leads to qualitative differences in different types of hay which are reflected in the price. Additionally, the claim that mountain hay, grown at altitudes above 1700 m, is outstandingly suited for this cure caused an almost incredible valorisation of this agricultural product (2.20 € + VAT/kg).

Unfortunately the brittleness [4] of hay after the haying complicates the botanical determination of single plants, which would allow inferences to the phytosociology which is characteristic for a meadow and thus for the hay's origin. Because of this circumstance hay of minor value, such as normal hay (harvested below 1700 m) or aftermath (2nd cut), can be sold at higher prices too, ignoring the high standards of production required to obtain a botanical certificate, which can be issued only after an inspection of the meadow before mowing.

Many strategies for the analysis of gas mixtures, such as the odour of hay [9], and their components include concepts for the enrichment of the volatile analytes. Beside classical solvent extractions or variants of headspace sampling, primarily the highly sophisticated adsorption to a fibre coated with an extraction phase [10] is a well-established technique for the sample preparation. Among these concepts especially the solid phase micro extraction [11] in the headspace mode (HS-SPME) in combination with hyphenated separation methods (e.g. GC-MS) should be pointed out, which owing to the high selectivity and efficiency of the available fibres is used in a number of applications for the analysis of environmental samples [12], food [13,14] and fragrances [15].

The automation of these important, and often necessary, preconcentration steps in the headspace has contributed significantly to the reduction of the time of analysis and cost of such analytical concepts for volatile analytes [16]; however, generally they are not yet considered as quick methods, because the sample throughput in many cases is still comparatively small and a real-time monitoring is not possible. Such applications are still a domain of gas sensors and e(lectronic)-noses [17]. Particularly the latter have shown their potential to solve a variety of problems in areas such as the manufacturing and quality control of food [18], environmental monitoring [19–21] or medical diagnostics [22,23]. This versatility of electronic noses for the detection and discrimination of complex odours is owed to the flexibility of the employed sensor arrays, which predominantly consist of conductometric chemosensors (metal-oxide semiconductors/MOS, conducting polymers), chemocapacitors, potentiometric chemosensors (e.g. MOS field-effect transistors), gravimetric chemosensors, surface acoustic wave (SAW), optical chemosensors, calorimetric sensors or amperometric sensors. Besides issues such as drift and its compensation [24,25], the selection of a suited sample preparation or sensitivity, the most challenging aspect when operating an electronic nose is probably the complexity of the acquired sensor response data which requires a sophisticated strategy for the evaluation [26], which may include e.g. multivariate statistical approaches or artificial neural networks (ANNs). This is especially true for the analysis of natural products with their inherent variability (origin, season, species).

Mass spectrometry is an important tool for quality control and in this context it has become an indispensable instrument for the analysis of a variety of natural products [27], profiting especially from the combination with separation techniques such as chromatography or electrophoresis. In the form of so-called *mass sensors* it has also emerged as a promising approach for e-noses, which are therefore sometimes referred to as new-generation electronic noses. Such instruments [28,29] are designed for a direct introduction of volatile compounds into an ionization chamber of a mass spectrometer without a prior separation. The registered fragment ions of the mass spectrum with their specific m/z ratio operate as sensors and their abundance is equivalent to a sensor signal. Hence MS-based e-noses can have a flexible number of sensors, which eventually provide interpretable chemical information about a sample through the fragmentation pattern. Especially innovative soft ionization techniques, such as the proton transfer reaction (PTR) ionization, have shown to be appropriate methods for the analysis of volatile organic compounds (VOCs) resulting from urban lawn mowing [30], agricultural grasslands [31] or herbal extracts [32], mastering successfully tasks similar to the one investigated here.

The goal of the present study was the development of a cheap and quick method, which enables the traceability of hay samples to their site of production. The V&F AirSense® technology, a spectrometer based on ion molecule reactions (IMR) [33] of mercury, xenon and krypton [34–36], fulfils the first two requirements. Its suitability for the problem at hand was evaluated using concepts of multivariate statistics [37,38] (PLS, PCA, SIMCA) for the interpretation of the acquired data.

2. Experimental

2.1 *Instrumentation*

The V&F (Andreas Hofer Strasse 15, A-6067 Absam, Austria) AirSense® is a quadrupole mass spectrometer equipped with a channeltron, which was designed for the quick analysis of gas mixtures [39] applying a proprietary system for the direct introduction of sample gases into the ionization chamber. It is based upon a special ionization technique, the ion molecule reaction (IMR). This variant of the chemical ionization [40], which generates just a few or even no fragments and can be run at different pressures [41], uses low-energy primary ions of mercury, krypton or xenon for a soft charge transfer to gaseous sample molecules.

The ion molecule reaction in the AirSense® occurs while the reactant gas ions of mercury, krypton or xenon are present in excess and the collision of such a positively charged ion, R^+, with a neutral analyte molecule, M, leads to a charge transfer which can be drafted in the following way:

$$R^{+\bullet}+M \rightarrow R + M^{+\bullet} \tag{1}$$

The unfragmented molecular ion $[M^{+\bullet}]$ is a radical because of the unpaired electron. This ion molecule reaction (IMR) is exothermic, if the recombination energy (with an electron) of the reactant ion $R^{+\bullet}$ is higher than the ionization potential of the neutral analyte molecule M. The exothermicity of the charge exchange reaction proves to remain primarily in a transition state as internal energy [42] in the product ion $M^{+\bullet}$. If this internal energy is high enough, a fragmentation of the product ion can be induced. The fragmentation reactions taking place are similar to those observed in electron impact ionization. However, while the molecular ions formed after electron impact are characterized by a distribution of their internal energy, ions resulting from the IMR, $M^{+\bullet}$, show a discrete amount of energy or are distributed in a small energy band, if reactant gas ions $R^{+\bullet}$ with more recombination energies are applied (e.g. the ground states of the singly charged noble gas ions are doublet states with configurations $^2P_{3/2}$ and $^2P_{1/2}$). The internal energies of ions formed in such ion-molecule reactions, $M^{+\bullet}$, are determined by the exothermicity of the charge exchange reaction. Since this exothermicity depends from the recombination energy of the selected reactant gas [35], R, and the ionization potential of the analyte molecule, M, the choice of the primary gas and thus of a characteristic recombination energy is a selectivity-determining factor, because it is decisive if, or to what degree, fragmentations are observed in the mass spectrum. The AirSense® provides the use of mercury (10.44 eV), xenon (12.12 eV) and krypton (13.99 eV) as possible primary gases.

It is important that the ionization potential of the primary ions (Hg, Xe, Kr) is sufficiently high to contribute to the ionization of the sample molecules. Their internal energy should be only slightly above (preferably $\leq$2 eV) the energy that is required to generate product ions, if the molecular peak of the substance of interest shall be investigated in the mass spectrum. Furthermore the employed primary gas ions should have a translational pulse energy of such an amount (preferably below 10 eV) in the respective centre-of-mass system that the kinetic effect on the ionization process is negligible in comparison to the influence of the internal energy. The reader interested in these aspects is referred to a V&F patent, wherein the inventors of the AirSense® technology discuss these issues [43].

2.2 *Methods*

An aqueous 100 mg L^{-1} solution of coumarin was prepared, 1 mL was given into a GC vial and thermostated at 60°C. The solution was then measured with the AirSense® using a scan set-up in the range from m/z 40 to m/z 170 setting the inlet pressure to 25 hPa. All possible primary gases (Hg, Kr, Xe) were used to see the behaviour of this well known analyte of hay in the IMR mass spectrometer.

Aqueous 10 mg L^{-1} solutions of the monoterpenes limonene, camphene and β-pinene as well as of p-cymene were measured with all ionization gases at 30°C and an inlet pressure of 25 hPa generating a spectrum ranging from m/z 40 to m/z 170. All these compounds are known components of hay too.

All hay samples were ground with a Fritsch (Idar-Oberstein, Germany) power cutting mill Pulverisette 25 using the 1.0 mm sieve cassette, cooling both stationary and rotating knives with compressed air thus minimizing loss of volatile analytes. After grinding the hay was stored in glass containers.

A total of 1.0 g of the ground hay was given into a GC vial and covered with untreated glass wool to avoid an obstruction of the tight transfer channel into mass spectrometer with dust. The sample was then thermostated for 30 min at 30°C in the heating block of the AirSense® sampler. This temperature was clearly preferred in comparison with a temperature of 50°C, which was also tested in a preliminary experiment to monitor selected signal intensities (a hay sample was spiked with 10 µl of water and measured with a provisional set-up at 30°C and 50°C), because of the lower influence of the vapour pressure of water, which could be in the hay even after the drying, with respect to the mass spectral signals (since too high intensities could eventually damage the detector or induce a drift). The inlet pressure was set to 25 hPa and the sample was finally measured with a combined set-up of xenon and mercury ionization. The applied scan sequence began with 31 xenon parameters (control mass CM 7 Xe, m/z: 7; 16; 20; 26; 27; 29; 41; 46; 47; 60; 64; 68; 69; 76–78; 90–92; 94; 104–107; 118–121; 145; 146; control mass CM Xe2*) and terminated with 188 mercury measuring points (control mass CM 7Hg, m/z: 17; 19; 28; 30–34; 37; 42–44; 46; 46–49; 54; 56; 57; 60; 60–63; 66–144; 147–166; 169–192; 208–219;

222–237; 240–249; control mass CM Hg2). Four cycles were used to measure the spectrum of a hay sample. During all measurements drift was monitored using a freshly prepared 10 mg L^{-1} aqueous solution of 1,2-Dichlorobenzene. However, owing to the stability of the system a drift correction has not been applied.

This set-up was also used to measure aqueous solutions of p-cymene (0.5, 1.0, 10 and 20 mg L^{-1}, 4 repetitions/sample) in order to compare an uni- and a multivariate calibration of a characteristic hay compound.

Microsoft Excel (Redmond, WA, USA) was used to create the depicted mass spectra and to calculate the results of the univariate calibration. Multivariate data analysis was performed employing Camo Unscrambler (Oslo, Norway).

2.3 *Samples and materials*

In total 136 samples including hay and aftermath from Poland (1), Germany (1), Switzerland (7), Austria (16) and Italy (111) were available. This sample set consisted of 40 mountain hay samples, 75 normal hay samples and 21 aftermath samples. The Austrian hay was provided by the Tiroler Landwirtschaftskammer (Brixner Straße 1, A-6020 Innsbruck), the German hay sample by the Landschaftspflegeverband Birkenfeld (Kreisverwaltung Birkenfeld, Untere Landespflegebehörde, D-55765 Birkenfeld). The Polish hay sample and a few Italian samples were obtained through private contacts. The biggest part of the Italian samples came from the Südtiroler Bergwiesenheugenossenschaft (Schlattach Niederstein 6/A, I-39015 St. Leonhard in Passeier), others from the agricultural institute San Michele all'Adige (Via Edmondo Mach 2, I-39010 San Michele all'Adige). The Swiss samples were ordered at Landi Wiggen (Alte Post, CH-6192 Wiggen). All samples were mowed in the same year and stored at room temperature in paper bags in a dry and dark room to avoid fermentation induced by humidity or light.

All chemicals used (analytical degree) were purchased from Sigma Aldrich (St. Louis, MO, USA).

3. Results and discussion

The effect of the AirSense® ionization technology on hay analytes can be studied directly comparing the recorded spectra with reference spectra and analysing appearing fragmentations. Figure 1(a) shows the base peak scaled AirSense® spectrum of an aqueous solution of coumarin using mercury for the ionization. The base peak appears at m/z 146 thus matching the nominal mass of coumarin and allowing a simple identification of this compound since all other intensities are rather low. The signal group formed around this characteristic mass-to-charge ratio is partly result of the limited resolution of the AirSense® ($R_{max} = 100$) leading to fuzzy intensities above m/z 100.

Figure 1(b) shows the spectrum of coumarin using xenon for the ionization under the conditions described in the experimental section. The ionization energy of xenon is higher than the ionization energy of mercury. Therefore higher intensities at lower m/z may be expected and in this case the base peak can indeed be found at m/z 118. However, the signal group around m/z 146 can still be observed. Both signals can also be found in the electron impact mass spectrum of coumarin depicted in Figure 1(c), which was taken from Wiley's NIST/EPA/NIH 2002 mass spectral library. The peak at m/z 118 could be the result of an ionization of the double-bound oxygen (lone pair electrons) of the δ-lactone

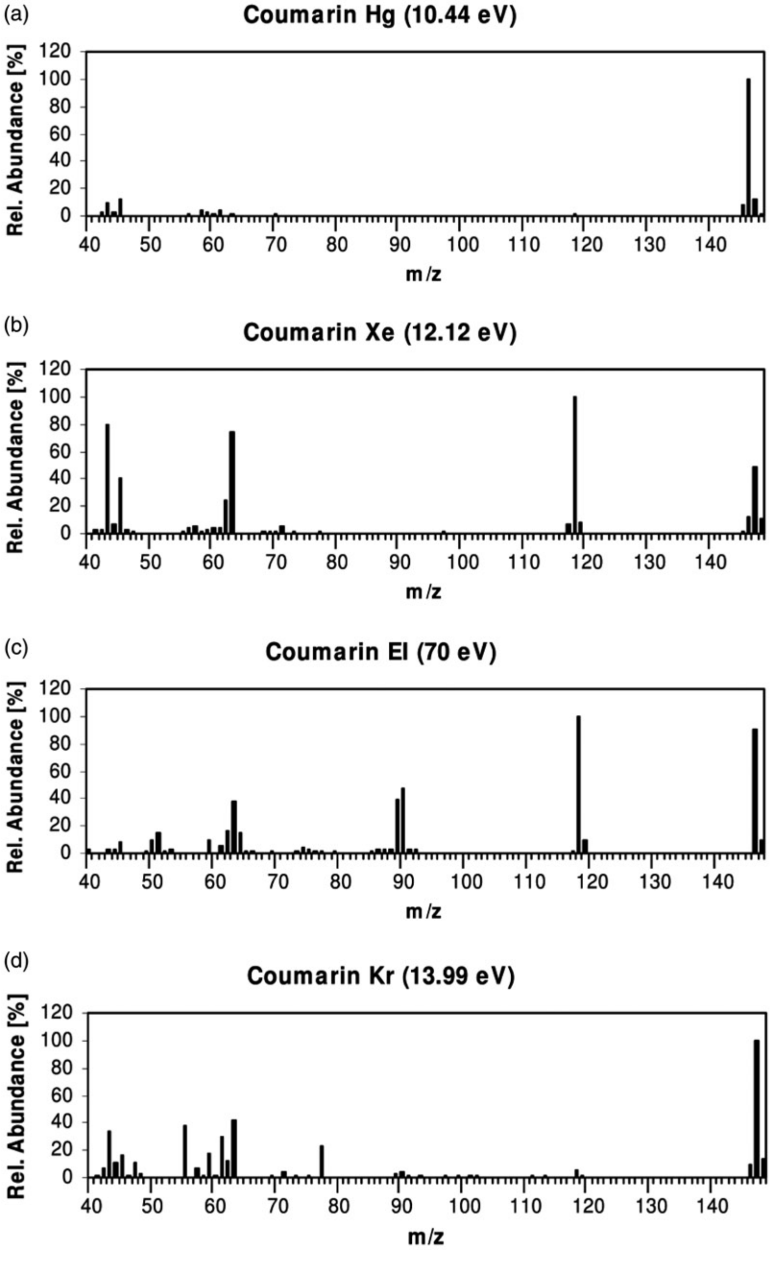

Figure 1. (a) AirSense® spectrum of an aqueous solution of coumarin using mercury as ionization gas, (b) AirSense® spectrum of an aqueous solution of coumarin using xenon for the ionization, (c) Electron impact spectrum of coumarin at 70 eV from Wiley NIST/EPA/NIH mass spectral library 2002, courtesy of NIST, (d) AirSense® spectrum of an aqueous solution of coumarin using krypton as ionization gas.

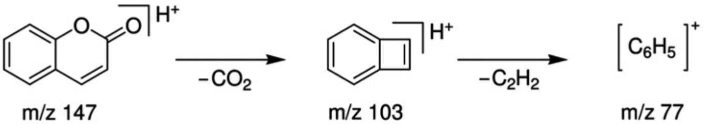

Figure 2. ESI-MS^n fragmentation pattern proposed for coumarin by Concannon *et al.* [59].

system in coumarin (m/z 146), followed by an α-cleavage and a subsequent elimination of CO (−28 m/z) leading to a cation detectable at m/z 118. The structure of this ion, especially whether it is a closed ring or not, as well as a variety of thermodynamic and kinetic aspects were investigated and discussed with more sophisticated approaches [44–48], but – at least to the authors' knowledge – no final conclusions were possible.

Figure 1(d) shows the mass spectrum of coumarin using the krypton ionization. The signals between m/z 78 and m/z 87 had to be suppressed because of the krypton isotopes (^{78}Kr, ^{80}Kr, ^{82}Kr, ^{83}Kr, ^{84}Kr, ^{86}Kr) which are present in excess, thus bearing no structural information, and could therefore damage the channeltron. Krypton has the highest ionization energy (13.99 eV) and therefore leads to spectra leaning to the left and lower m/z when compared with xenon and mercury spectra. While the base peak is now at m/z 147, the relative intensity of the peak at m/z 118 is considerably lower. These findings could indicate an additional mechanism for this fragmentation pattern.

Very fast and efficient charge transfer reactions (2) between $Kr^{+\bullet}$ and H_2O, which is omnipresent – at least in traces – in hay and has an ionization potential of 12.6 eV (lower than that of Kr), are well studied and lead to the production of $H_2O^{+\bullet}$ ions [49–52], which then rapidly react with H_2O (3) [53,54]. The resulting H_3O^+ ions (and clusters thereof) are suited precursors [55] to undergo efficient proton transfer reactions (PTR) with molecules, which have proton affinities greater than that of water molecules, thus finally producing $[M+H]^+$ ions [56–58]. In the case of coumarin this should lead to the aforementioned peak at m/z 147.

$$Kr^{+\bullet} + H_2O \rightarrow H_2O^{+\bullet} + Kr \tag{2}$$

$$H_2O^{+\bullet} + H_2O \rightarrow H_3O^{+} + HO^{\bullet} \tag{3}$$

A sophisticated ESI-MS^n based investigation about the fragmentation of coumarin derivatives was performed by Concannon *et al.* [59], who proposed the interpretation depicted in Figure 2. In contrast with the EI induced fragmentation [60], their approach, which includes a protonation, would involve as a first step the expulsion of CO_2 from the pyrone ring system, which would consequently lead to a strained protonated bicyclic ring detectable at m/z 103. The further fragmentation, which should include the loss of acetylene, C_2H_2, would then result in a product ion that should be registered at m/z 77. Our experimental results could agree with this report, since we were able to find the peaks at m/z 147 (100%) and m/z 77 (23%) with acceptable relative abundances, but the peak at m/z 103, eventually representing the (deloc-1,2,3,5,6,7,8)-Bicyclo[4.2.0]octa-2,5,7-trien-1-ylium cation from Figure 2, shows a rather low intensity (1.6%), which could be the result of its poor relative stability. The reader interested in this ion is referred to a theoretical work by Eckert-Maksić *et al.* [61], who performed ab initio HF 6-31G* and MP2(fc)/6-31G*//HF/6-31G* calculations, in order to study electronic and geometric structures and to discuss energetic aspects.

These results indicate that a combined set-up involving mercury ionization (molecular peak) and at least another ionization gas (fragmentation) is best suited to filter structural information from the mass spectra. To reduce the measurement time and complex enrichment processes in the gas mixture a set-up with only two ionization gases is preferred. The present case study shows that the medium ionization energies from xenon suffice to observe the fragments of coumarin known from the EI spectrum.

The mercury AirSense®-spectra of the monoterpenes limonene, camphene and β-pinene are depicted in Figure 3, the relative abundances of important fragments are detailed in Table 1. The bicyclic terpenes camphene and β-pinene with their exocyclic double-bonds do not show a distinctive molecular peak, but the monocyclic limonene with two double-bonds competing for a π-ionization features a signal group around m/z 136 including the molecular peak. The comparison in Figure 3 indicates that an isomeric discrimination of these compounds in a mixture, based on relative intensities only, is hardly feasible, because of a number of common fragments, and therefore requires the involvement of a multivariate pattern analysis method, such as the principal component analysis (PCA). A report of Steeghs *et al.* [62] about the dissociation patterns of 10 monoterpenes, among them limonene, camphene and β-pinene, in an attempt to distinguish between different monoterpenes confirms the difficulty of this task, especially when investigating gas mixtures of these compounds. Similar conclusions were drawn in a PTR-MS study about these monoterpenes, where Maleknia *et al.* [63] suggest the loss of neutrals as an explanation for the observed fragmentation pattern, which should agree with the fragments described in Table 1 (m/z 120:–CH_4, m/z 108: –C_2H_4, m/z 106: –C_2H_6, m/z 94: –C_3H_6, m/z 92: –C_3H_8), and report about electron impact spectra of these monoterpenes with the ions $C_7H_9^{+\bullet}$ (m/z 93) and $C_7H_{11}^{+\bullet}$ (m/z 95), which can also be found in Table 1. Additionally, the ionization of those small molecules, which result from the fragmentation of the pure compound, within the reaction chamber could contribute significantly to the complexity of the spectrum of such a gas mixture. For instance, the camphene spectrum in Figure 3 therefore shows high intensities at the left side of the spectrum, which should result from the ionization of C_3H_8 (m/z 44) and C_3H_6 (m/z 42).

Figure 4 shows the mercury AirSense®-spectrum of p-cymene. This compound, often appearing in hay [5], has a nominal mass of 134 thus not belonging to the monoterpenes, which have the general molecular formula $C_{10}H_{16}$ and a nominal mass of 136. The molecular ion of this compound is rather stable and can easily be observed with a relative abundance of 14.9%. The limited resolution of the AirSense® above m/z 100 however complicates the separation from the class of monoterpenes (regions around m/z 135 and 120 in the spectra of limonene and p-cymene) and this is a crucial aspect for data mining. The application of the first derivative is a suited data pre-treatment method to deal with overlapping spectra in multivariate approaches [64] enhancing discrimination power.

Because of its high frequency in hay [5], p-cymene was also used to verify the suitability of the combined mercury and xenon set-up outlined in the experimental section to quantify such a characteristic VOC of hay. The classical approach of an univariate calibration [65] based on single peaks was performed using the molecular peak at m/z 134 and the base peak at m/z 119 (loss of a methyl group, $\Delta m = 15$) from the mercury part of the spectrum. The figures of merit of the signals m/z 134 ($LOD = 3.68\,mg\,L^{-1}$, $LOQ = 5.11\,mg\,L^{-1}$, $R^2 = 0.982$, $P = 99\%$) and m/z 119 ($LOD = 0.86\,mg\,L^{-1}$, $LOQ = 1.26\,mg\,L^{-1}$, $R^2 = 0.999$, $P = 99\%$) indicate that the base peak at m/z 119 is, as expected, better suited for a calibration with respect to the limit of detection (LOD), to the limit of quantitation (LOQ) and to linearity, however these results would suggest that this set-up (Xe&Hg), which had

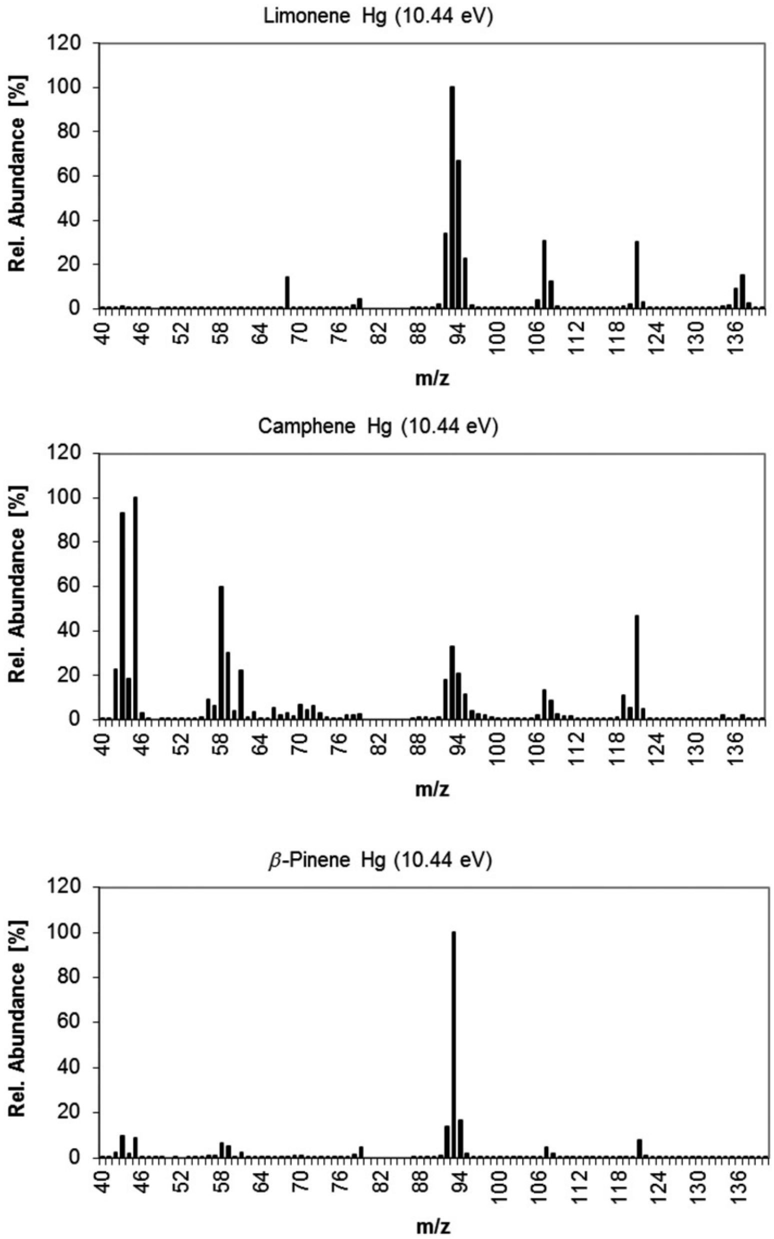

Figure 3. AirSense® spectra of limonene, camphene and β-pinene using mercury ionization.

not been optimised for this purpose but for its classification ability, and the calibration range (0.50–20.00 mg L^{-1}) are only moderately suited to prepare an univariate quantitation.

In a further study a PLS1 (partial least squares) calibration, a multivariate bilinear modelling method [66], was performed using the signals of the combined mercury and xenon spectrum as predictor variables (219 variables). The data set was not pre-treated.

Table 1. Relative abundances of important fragments in AirSense® spectra of 100 mg L^{-1} aqueous solutions of the monoterpenes limonene, camphene and β-pinene using an inlet pressure of 25 hPa and mercury for the ionization (further details can be found in the text).

m/z	Limonene [%]	Camphene [%]	β-pinene [%]
92	34.2	18.2	14.0
93	100.0	33.0	100.0
94	67.0	20.8	16.5
95	22.8	11.3	1.8
106	3.7	1.8	0.6
107	30.6	13.3	4.5
108	12.6	8.7	2.0
109	1.1	2.3	0.2
120	2.2	5.4	0.6
121	30.0	46.8	7.8
122	3.2	4.6	0.9
136	9.1	0.3	0.3

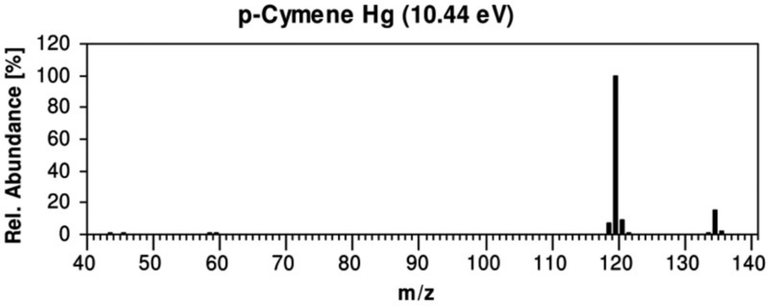

Figure 4. AirSense® spectrum of an aqueous solution of p-cymene using mercury as ionization gas.

The results of the regression obtained with the Unscrambler software were tested using a full (leave-one-out) cross validation to determine a suited number of principal components (PC) for this task considering the following aspects discussed by Esbensen [38]: (a) the root mean square error of the prediction (RMSEP) should be small, preferably in a minimum when plotted against the number of principal components, (b) simple models with fewer principal components were preferred. Therefore the model with three principal components ($R^2 = 0.998$), which showed a minimum for the RMSE (fulfilling condition (a), Figure 5(a)) and is able to explain 99.85% of the response variable variance with 99.79% of the variance in the spectra (contributing to a lower model complexity), was used to estimate the limit of determination. For this purpose a Matlab package for multivariate calibration (MVC1) developed by Olivieri *et al.* [67] was employed. Both the limit of determination (defined as 3^*s_R/Sensitivity = 0.13 mg L^{-1}, s_R is the standard deviation of the instrumental response) and the limit of quantitation (defined as 10^*s_R/Sensitivity = 0.42 mg L^{-1}) were, as expected for a multisensor method [68], lower than for the classical approach profiting from correlation effects and the relative reduction of

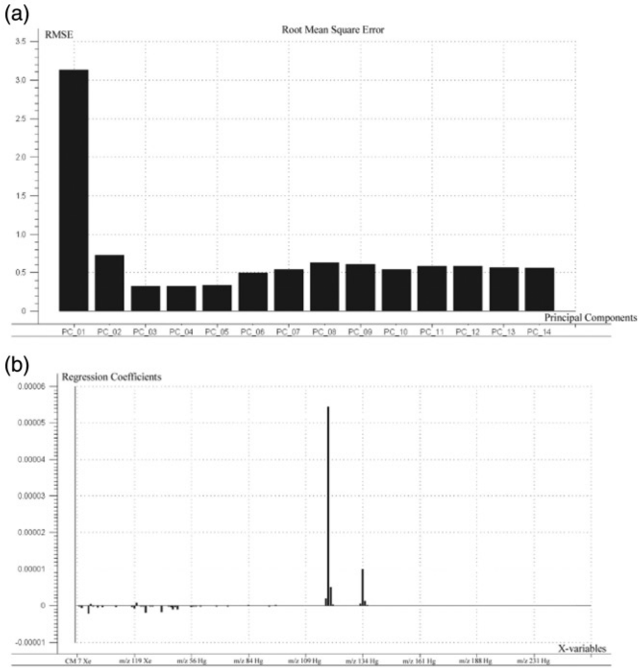

Figure 5. Aspects of the PLS1-Regression: (a) showing the root mean square error (RMSE) plotted against the number of principal components with a minimum at the 3rd principal component, (b) showing the regression coefficients for the model with three principal components, dominated by the signals M134 (mol peak of p-cymene) and M119 (loss of a methyl group) in the mercury part of the combined spectrum.

noise [69]. The highest regression coefficients resulted from the M119 and M134 signals from the mercury part of the combined spectrum (Figure 5(b)) which correspond to base peak and molecular peak in the p-cymene spectrum (Figure 4).

This confirms that the lower end of the calibration range, $0.5\,\mathrm{mg\,L^{-1}}$, is accessible for this set-up of the AirSense®, even without pre-processing the spectra or specifying a spectral window. This finding also shows that a typical compound of hay, such as p-cymene, can be integrated in a qualitative model (e.g. for a classification) even if present in low concentrations only. A quantitative estimation of single hay compounds, however, was not performed using this approach, but can be found along with the relative frequency of known volatile hay constituents in a previous study of the authors [5].

Thereby also volatiles with higher molecular masses such as oxidized sesquiterpenes (e.g. caryophyllene oxide, $\mathrm{M} = 220.35\,\mathrm{g\,mol^{-1}}$) had been found. Therefore the measurement range of the AirSense® set-up with mercury as ionization gas was expanded up to m/z 250, in order potentially to include molecular peaks and fragments of these substances, which owing to their partly low occurrence in the studied hay samples contribute to the characterization of single hay samples. The aforementioned GC-MS approach had also shown that a number of sesquiterpenes (among them: β-bourbonene; γ-selinene; epi-bicyclosesquiphellandrene; ylangene; cyclosativene; β-cubebene; α-caryophyllene; γ-muurolene; β-farnesene; β-elemene; copaene and β-caryophyllene) with the molecular formula $C_{15}H_{24}$ and a molecular mass of $204.35\,\mathrm{g\,mol^{-1}}$, which may be found in the hay samples. Their molecular peaks unfortunately cannot be detected, because the range between m/z 193 and m/z 207 had to be excluded from the set-up due to potentially damaging effects of mercury isotopes (^{196}Hg, ^{198}Hg, ^{199}Hg, ^{200}Hg, ^{201}Hg, ^{202}Hg, ^{204}Hg).

Therefore in order to study the traceability of single types of hay, each of the 136 samples was measured 10 times using the combined xenon and mercury set-up of the AirSense® presented in the experimental section. The ten spectra obtained for each hay sample were then used to make a characteristic multivariate model based on a principal component analysis (PCA). For that reason the data set for each hay had to be pre-treated as follows: the first-order derivatives for the spectra were calculated using an algorithm implemented in the Unscrambler software (Norris, Segment size for averaging: 3, $\Delta(x_k - x_{k-1})$:2), the data set was centred and the variables were standardized, which is helpful to avoid an overemphasis of intense signals. The results of each PCA were validated with a full cross validation.

To check the suitability of the PCA models to characterize the single types of hay, nine randomly selected samples of mountain hay, three randomly selected samples of aftermath and three randomly selected samples of 'normal' hay were measured three times with the xenon and mercury set-up. The obtained spectra were then used for a classification attempt. For this purpose SIMCA (Soft Independent Modelling of Class Analogy), a classification method based on disjoint PCA models [70], was employed. It tries to model similarities between members of the same class and to recognize unknown samples as members of a class, if they are similar enough, else rejecting them. The significance level for this task was set to 0.05, the optimal number of PCs for each PCA-model was derived from the cross validation.

While this approach was successful for the correct and smooth classification of mountain hay samples (25/27, i.e. 93% correctly classified, 2% false positives), the results for both 'normal' hay (6/9, i.e. 66% correctly classified, 15% false positives) and aftermath (0/6, i.e. 0% correctly classified, 13% false positives) indicate that it is not suited for the latter types of samples (Table 2). The good results for mountain hay could be caused by

Table 2. Classification results for different kinds of test samples.

Hay sample	Type of hay	Cut	Altitude [m]	Correctly classified
A03	Mountain hay	1	1750	3 of 3
P59	Mountain hay	1	2000	2 of 3
P80	Mountain hay	1	1900	3 of 3
P81	Mountain hay	1	2100	3 of 3
P82	Mountain hay	1	2000	3 of 3
S19	Mountain hay	1	1900	2 of 3
S43	Mountain hay	1	1973	3 of 3
S49	Mountain hay	1	2500	3 of 3
S52	Mountain hay	1	2100	3 of 3
P08	Hay	1	600	1 of 3
P09	Hay	1	630	3 of 3
P50	Hay	1	1130	2 of 3
P51	Aftermath	2	1130	0 of 3
P23	Aftermath	2	650	0 of 3
P70b	Aftermath	2	1250	0 of 3

the fact that homogenizing manure is excluded for mountain meadows, thus allowing the formation of phytosociological units typical for climate and soil [71,4]. The resulting biodiversity should then lead to a variety of VOCs detectable with the AirSense®, which form a characteristic spectral pattern for these samples, ideal for discrimination and hence for traceability. A comparison of the results for the samples P50 and P51 in Table 2 also evidences the importance of biodiversity for a correct classification. Both of them originate from the same meadow, but while the hay P50 can still be identified reasonably (in 2 of 3 cases), this is not possible at all for the aftermath P51. After the first cut (hay), which comprises a bigger number of plant species (those growing and blooming between spring and early/mid summer), the second cut (aftermath) includes fewer plants, because they grow afterwards and in the shorter period until early autumn.

In order to give a visual impression of the discrimination power to distinguish between single samples of hay using the selected AirSense® set-up (mercury and xenon for the ionization) and the employed data pre-treatment (Norris derivative, data set standardization) a concrete example with a three-dimensional scores-plot (with the first three principal component axes) of a cross validated principal component analysis of three samples from South Tyrol (P80, P81, P82) and a sample from Austria (A03) is depicted in Figure 6. The model was created using 10 AirSense®-spectra (an example for an untreated digitized composite xenon and mercury spectrum of the hay sample A03 from Austria is given in Figure 7; the intensities of the single signals depend from the position in the

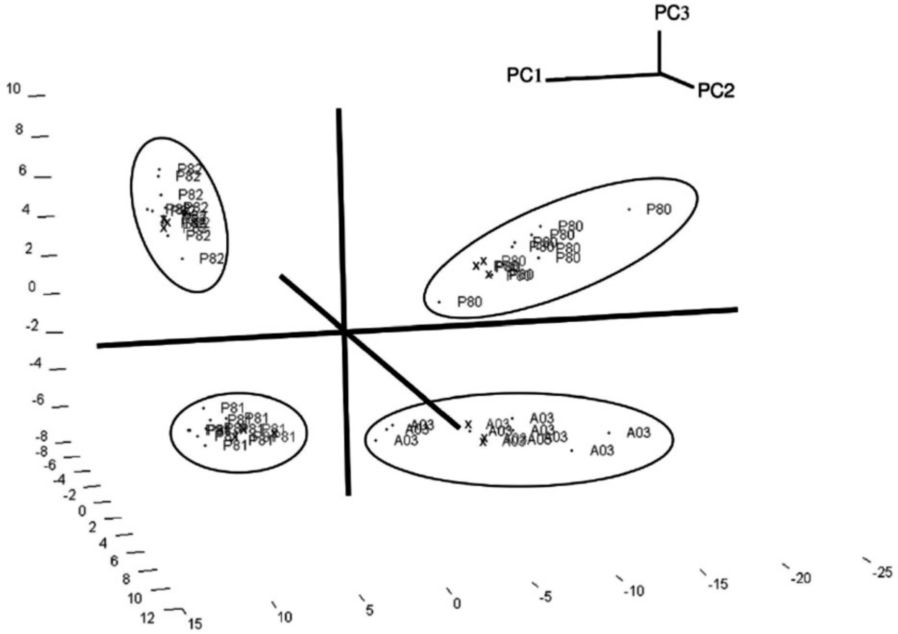

Figure 6. PCA scores plot with three principal components involving four hay samples: the clusters for each hay sample are compact and distant enough to allow an easy discrimination between single hay samples under the selected conditions for measurement (Xe and Hg ionization) and data-pretreatment (Norris derivative, data set standardization). The test samples (marked x) fall within the corresponding clusters.

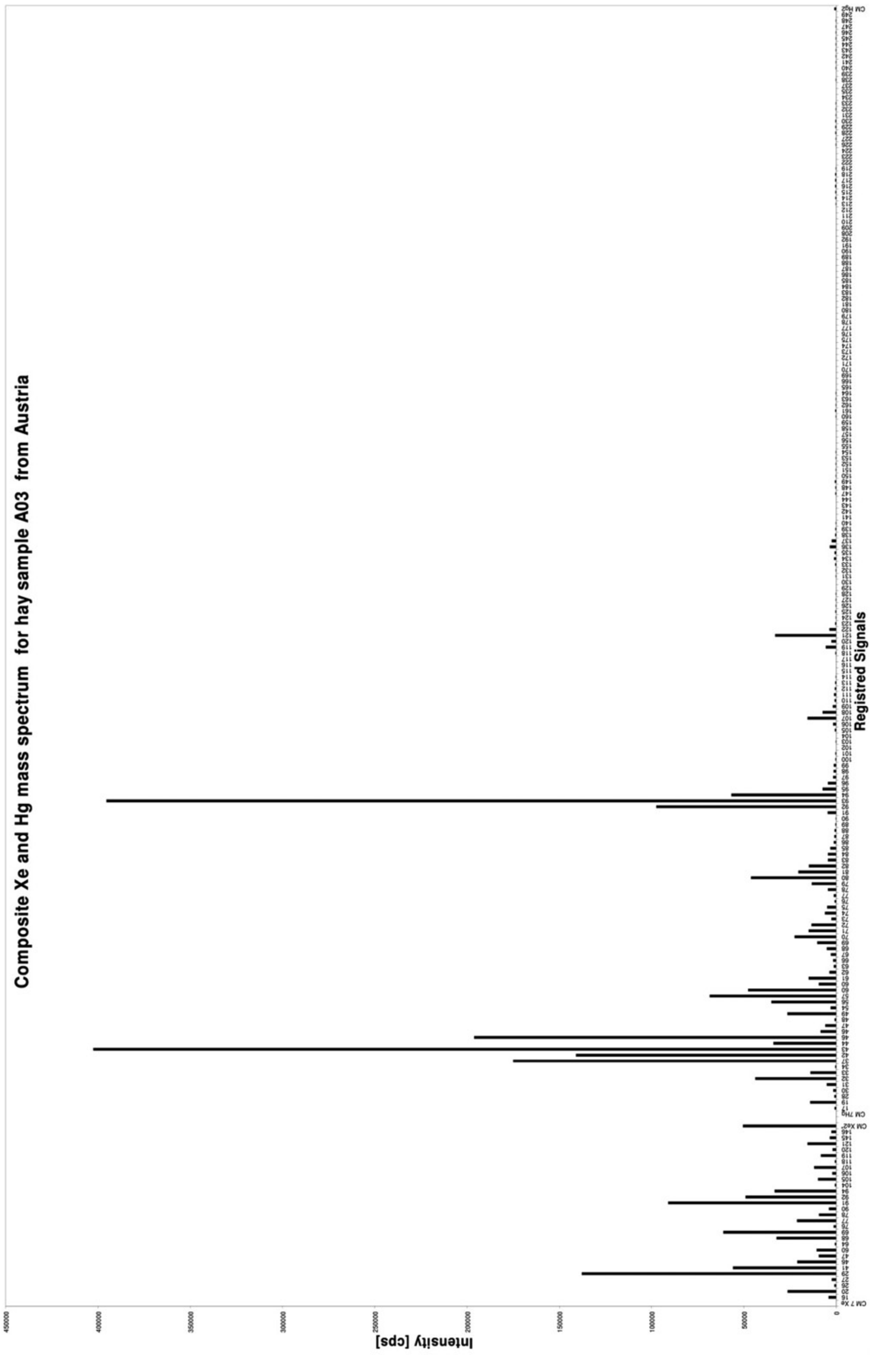

Figure 7. Example of a composite mass spectrum of a hay sample using xenon and mercury for the ionization. Temperature: 30°C, inlet pressure: 25 hPa.

Table 3. Model distances between the described (see text) PCA-models of the hay samples A03, P80, P81 and P82, calculated with the Unscrambler. The number in parenthesis refers to the number of principal components used for the specified model (derived from a full Cross validation) in the SIMCA analysis.

Model	A03 (5)	P80 (5)	P81 (8)	P82 (4)
A03	1	2658.31	8698.23	49185.62
P80	2658.31	1	28808.26	70197.09
P81	8698.23	28808.26	1	6426.34
P82	49185.62	70197.09	6426.34	1

measurement cycle, from the compounds' vapour pressure as well as the presence of compounds which could eventually influence the complex gas phase equilibrium) without the control masses for each of the four hay samples. For pre-treatment the data set, which consists of the first-order Norris derivatives (Segment size for averaging: 3, $\Delta(x_k - x_{k-1}) : 2$) of the spectra, was centred and the variables, i.e. the single signal intensities, standardized. The resulting four clusters in the PCA scores-plot (Figure 6) with the first three principal components (which can explain 74% of the total variance according to the leave-one-out cross validation) can be used to give an orientation to which group unknown samples belong. To show this, three test samples (marked x in Figure 6) for each of the single types of hay employed in this exemplification were projected into the selected subspace spanned by the first three principal components. As can be seen in Figure 6 these test samples can be attributed easily to the corresponding cluster to which they actually belong. This is possible because the single clusters which represent such a hay sample are rather compact and far enough from each other to avoid an interference.

The model distances between the PCA models of the hay samples A03, P80, P81 and P82, which were used for the SIMCA analysis, are given as a matrix in Table 3. Following the useful rule-of-thumb reported by Esbensen [38] which suggests that model distances greater than 3 indicate significant model differences, it shows that the PCA-models of A03, P80, P81 and P82 are clearly separable since all model distances are far above 3.

4. Conclusions

This mass spectral approach for the analysis of characteristic volatiles of hay, such as coumarin or monoterpenes, shows that these compounds can easily be measured using selected ion-molecule reactions in a mass spectrometer designed for this purpose. In comparison with near-infrared spectroscopy (with typical limits of detection in the lower percentage range), nowadays a standard method to accomplish quick analyses of agricultural products [72] and food, it should be pointed out that the sensitivity of the measurement principle allows, as shown for p-cymene, low limits of determination for hay VOCs, which in combination with suited chemometric concepts should help to enhance discrimination power.

The presented strategy reveals its potential for a correct classification of mountain hay samples in a relatively short time (5 min for sample preparation, 30 min for thermostating, 20 min for the measurement of three samples and data analysis), but fails to achieve this target for 'normal' hay samples and aftermath samples. However, it should offer an easily accessible protection for those precious mountain hay samples, which were registered in a database, from forgeries (under these circumstances 'normal' hay or aftermath). Since neither solvents nor additional chemicals are needed to perform a classification, it can be considered environment-friendly and cheap. This application confirms the broad analytical applicability for these types of IMR-spectrometers alongside classical areas of application such as medical sciences [42] or the automotive industry [73].

Acknowledgements

The authors would like to thank the Landesumweltagentur of the Autonomous Province Bozen-Südtirol for kind assistance. Moreover, we want to thank all of the farmers and agricultural institutions for providing hay samples and additional information about the meadows. Besides, we are grateful to Prof. Alejandro Olivieri (National University of Rosario, Department of Chemistry, Argentina) for his permission to use MVC1. We also would like to thank V&F Analyse- und Messtechnik GmbH (Absam, Austria) for the helpful suggestions and the quick support.

Furthermore, we would like to emphasize that this work would not have been possible without the help of the former head of the Department of Spatial Planning, Environment and Energy of the Autonomous Province of Bozen-Südtirol, Dr. Walter Huber, who organized the collaboration between Innsbruck and Bozen.

References

[1] L.U. Opara, J. Food Agr. Environ. **1**, 101 (2003).
[2] K. Sotriffer, *Heu & Stroh – Ein Beitrag zur Kultur und Kunstgeschichte* (Veritas, Linz, Austria, 1990).
[3] L. Hörmann, *Das Tiroler Bauernjahr, Jahreszeiten in den Alpen* (Wagner, Innsbruck, Austria, 1899).
[4] J. Dalla Via, E. Tasser, U. Tappeiner, S. Baric, V. Mair, and A. Kasal, Laimburg Journal **1**, 95 (2004).
[5] S.M. Valtiner, G.K. Bonn, and C.W. Huck, Phytochem. Anal. **19**, 359 (2008), DOI: 10.1002/pca.1062.
[6] H. Frass and F.H. Riedl, *Heilbäder und Heilwässer in Südtirol* (Athesia, Bozen, Italy, 1979).
[7] L. Jirovetz, G. Buchbauer, A. Nikiforov, G. Remberg, and V. Raverdino, Peak. Autumn, 4 (1989).
[8] B. Uehleke and H. Wöhling, Phys. Med. Rehab. Kuror. **14**, 97 (2004), DOI: 10.1055/s-2003-812649.
[9] G. Buchbauer, L. Jirovetz, A. Nikiforov, G. Remberg, and V. Raverdino, J. Ess. Oil Res. **2**, 185 (1990).
[10] W. Wardencki, J. Curylo, and J. Namiesnik, J. Biochem. Biophys. Meth. **70**, 275 (2007), DOI: 10.1016/j.jbbm.2006.07.004.
[11] J. Pawliszyn, *Solid Phase Microextraction in Theory and Practice* (John Wiley & Sons, New York, 1997).
[12] R. Zhao, X. Wang, J. Yuan, T. Jiang, S. Fu, and X. Xu, Anal. Bioanal. Chem. **384**, 1618 (2006), DOI: 10.1007/s00216-006-0341-5.
[13] M.S. Altaki, F.J. Santos, and M.T. Galceran, Talanta **78**, 1315 (2009), DOI: 10.1016/j.talanta.2009.02.003.
[14] G. Flamini, Curr. Anal. Chem. **3**, 149 (2007), DOI: 10.2174/157341107780361691.
[15] F. Maggi, T. Bilek, G. Cristalli, F. Papa, G. Sagratini, and S. Vittori, J. Sci. Food Agric. **89**, 2505 (2009), DOI: 10.1002/jsfa.3757.
[16] S. Risticevic, V.H. Niri, D. Vuckovic, and J. Pawliszyn, Anal. Bioanal. Chem. **373**, 781 (2009), DOI: 10.1007/s00216-008-2375-3.
[17] T.C. Pearce, S.S. Schiffman, H.T. Nagle, and J.W. Gardner, editors, *Handbook of Machine Olfaction* (Wiley-VCH, Weinheim, Germany, 2003).

[18] M. Peris and L. Escuder-Gilabert, Anal. Chim. Acta. **638**, 1 (2009), DOI: 10.1016/j.aca.2009.02.009.

[19] T. Sobanski, A. Szczurek, K. Nitsch, B.W. Licznerski, and W. Radwan, Sens. Actuators B **116**, 207 (2006), DOI: 10.1016/j.snb.2005.11.087.

[20] Q. Ameer and S.B. Adeloju, Sens. Actuators B **106**, 541 (2005), DOI: 10.1016/j.snb.2004.07.033.

[21] L. Capelli, S. Sironi, P. Centola, R. Del Rosso, and M. Il Grande, Sens. Actuators B **131**, 53 (2008), DOI: 10.1016/j.snb.2007.12.004.

[22] M. Bernabei, G. Pennazza, M. Santonico, C. Corsi, C. Roscioni, R. Paolesse, C. Di Natale, and A. D'Amico, Sens. Actuators. B **131**, 1 (2008), DOI: 10.1016/j.snb.2007.12.030.

[23] A. D'Amico, C. Di Natale, R. Paolesse, A. Macagnano, E. Martinelli, G. Pennazza, M. Santonico, M. Bernabei, C. Roscioni, G. Galluccio, R. Bono, E. Finazzi Agrò, and S. Rullo, Sens. Actuators B **130**, 458 (2008), DOI: 10.1016/j.snb.2007.09.044.

[24] M. Holmberg, F. Winquist, I. Lundström, F. Davide, C. Di Natale, and A. D'Amico, Sens. Actuators B **36**, 528 (1996), DOI: 10.1016/S0925-4005(97)80124-4.

[25] R. Ionescu, A. Vancu, and A. Tomescu, Sens. Actuators B **69**, 283 (2000), DOI: 10.1016/S0925-4005(00)00508-6.

[26] S.M. Scott, D. James, and A. Zulfiqur, Microchim. Acta **156**, 183 (2007), DOI: 10.1007/s00604-006-0623-9.

[27] F.K. Yeboah and Y. Konishi, Anal. Lett. **36**, 3271 (2003), DOI: 10.1081/AL-120026571.

[28] W. Cynkar, D. Cozzolino, B. Dambergs, L. Janik, and M. Gishen, Sens. Actuators B **124**, 167 (2007), DOI: 10.1016/j.snb.2006.12.017.

[29] D. Cozzolino, H.E. Smyth, W. Cynkar, R. G. Danbergs, and M. Gishen, Talanta **68**, 382 (2005), DOI; 10.1016/j.talanta.2005.08.057.

[30] T. Karl, R. Fall, A. Jordan, and W. Lindinger, Environ. Sci. Technol. **35**, 2926 (2001), DOI: 10.1021/es010637y.

[31] B. Davison, A. Brunner, C. Ammann, C. Spirig, M. Jocher, and A. Neftel, Plant Biol. **10**, 76 (2008), DOI: 10.1055/s-2007-965043.

[32] D. Jaksch, E. Hartungen, T. Mikoviny, G. Abel, and T.D. Märk, Int. J. Mass Spectrom. **239**, 203 (2004), DOI: 10.1016/j.ijms.2004.07.019.

[33] E.E. Ferguson, Annu. Rev. Phys. Chem. **26**, 17 (1975), DOI: 10.1146/annurev.pc.26.100175.000313.

[34] D. Smith, N.G. Adams, E. Alge, H. Villinger, and W. Lindinger, J. Phys. B: Atom. Molec. Phys. **13**, 2787 (1980), DOI: 10.1088/0022-3700/13/14/018.

[35] N.G. Adams, D. Smith, and E. Alge, J. Phys. B: Atom. Molec. Phys. **13**, 3235 (1980), DOI: 10.1088/0022-3700/13/16/020.

[36] K. Giles, N.G. Adams, and D. Smith, J. Phys. B: At. Mol. Opt. Phys. **22**, 873 (1989), DOI: 10.1088/0953-4075/22/6/013.

[37] R.G. Brereton, *Applied Chemometrics for Scientists* (John Wiley & Sons, Chichester, West Sussex, England, 2007).

[38] K.H. Esbensen, *Multivariate Data Analysis – In Practice* (Camo Process AS, Oslo, Norway, 2002).

[39] J. Villinger, W. Federer, W. Lubich, A. Weissnicht, and G. Sandstroem, presented at the 13th International Symposium on Clorinated Dioxins and Related Compounds, Vienna, Austria, September 20–24, 1993.

[40] M.S.B. Munson and F.H. Field, J. Am. Chem. Soc. **88**, 2621 (1966), DOI: 10.1021/ja00964a001.

[41] H.-H. Grotheer, N. Stothard, J. Villinger, and W. Federer, Deutsches Patent- und Markenamt Patent DE 19628093 (22 January 1998).

[42] C. Hornuss, S. Praun, J. Villinger, A. Dornauer, P. Moehnle, M. Dolch, E. Weninger, A. Chouker, C. Feil, J. Briegel, M. Thiel, and G. Schelling, Anesthesiology 106, 665 (2007).

[43] W. Federer and J. Villinger, US Patent No. 4,975,576 (December 4 1990).

[44] S.-Y. Tang, J.C. McGowan, M. Singh, P. Galatsis, B.E. Ellis, R.K. Boyd, and S.A. Brown, Can. J. Chem. **57**, 1995 (1979), DOI: 10.1139/v79-319.

[45] S.E. Drewes, in *Progress in Mass Spectrometry*, Vol. II., edited by H. Budzikiewicz (Verlag Chemie, Weinheim, Germany, 1974).

[46] R.A.W. Johnstone, B.J. Millard, F. Dean, and A.W. Hill, J. Chem. Soc. C **19**, 1712 (1966), DOI: 10.1039/J39660001712.

[47] F.M. Dean, J. Goodchild, R.A.W. Johnestone, and B.J. Millard, J. Chem. Soc. C **21**, 2232 (1967), DOI: 10.1039/J39670002232.

[48] J.L. Occolowitz and G.L. White, Aust. J. Chem. **21**, 997 (1968), DOI: 10.1071/CH9680997.

[49] C.J. Howard, H.W. Rundle, and F. Kaufman, J. Chem. Phys. **53**, 3745 (1970), DOI: 10.1063/1.1674558.

[50] R. Marx, G. Mauclaire, and R. Derai, Int. J. Mass Spetrom. Ion Phys. **47**, 155 (1983), DOI: 10.1016/0020-7381(83)87159-9.

[51] R.A. Dressler, S.T. Arnold amd, and E. Murad, J. Chem. Phys. **103**, 9989 (1995), DOI: 10.1063/1.469888.

[52] H.-S. Kim, C.-H. Kuo, and M.T. Bowers, J. Chem. Phys. **93**, 5594 (1990), DOI: 10.1063/1.459630.

[53] W.T. Huntress and R.F. Pinizzotto, J. Chem. Phys. **59**, 4742 (1973), DOI: 10.1063/1.1680687.

[54] R.C. Bolden and N.D. Twiddy, Faraday Discuss. **53**, 192 (1972), DOI: 10.1039/DC9725300192.

[55] D. Smith, A.M. Diskin, Y. Ji, and P. Španěl, Int. J. Mass Spectrom. **209**, 81 (2001), DOI: 10.1016/S1387-3806(01)00478-X.

[56] P. Španěl and D. Smith, J. Phys. Chem. **99**, 15551 (1995), DOI: 10.1021/j100042a033.

[57] E.P. Hunter and S.G. Lias, J. Phys. Chem. Ref. Data. **27**, 413 (1998).

[58] G. Bouchoux, J.Y Salpin, and D. Leblanc, Int. J. Mass Spectrom. Ion Proc. **153**, 37 (1996), DOI: 10.1016/0168-1176(95)04353-5.

[59] S. Concannon, V.N. Ramachandran, and W.F. Smyth, Rapid Commun. Mass Spectrom. **14**, 1157 (2000), DOI: 10.1002/1097-0231(20000730)14:14 < 1157::AID-RCM4 > 3.0.CO;2-V.

[60] Q.N. Porter, *Mass Spectrometry of Heterocyclic Compounds* (John Wiley & Sons, New York, 1985).

[61] M. Eckert-Maksić, W.M.F. Fabian, R. Janoschek, and Z.B. Maksić, J. Molec. Struct. (Theochem) **338**, 1 (1995), DOI: 10.1016/0166-1280(94)04043-R.

[62] M.M.L. Steeghs, E. Crespo, and F.J.M Harren, Int. J. Mass Spectrom. **263**, 204 (2007), DOI: 10.1016/j.ijms.2007.02.011.

[63] S.D. Maleknia, T.L. Bell, and M.A. Adams, Int. J. Mass Spectrom. **262**, 203 (2007), DOI: 10.1016/j.ijms.2006.11.010.

[64] T. Azzouz, A. Puigdomenech, M. Aragay, and R. Tauler, Anal. Chim. Acta **484**, 121 (2003), DOI: 10.1016/S0003-2670(03)00308-8.

[65] F.W. Küster and A. Thiel, in *Rechentafeln für die chemische Analytik*, edited by A. Ruland (Walter de Gruyter, New York, 2003).

[66] M. Otto, *Chemometrics – Statistics and Computer Application in Analytical Chemistry* (Wiley-VCH, Weinheim, Germany, 2007).

[67] A.C. Olivieri, H.C. Goicoechea, and F.A. Iñón, Chemom. Intell. Lab. Syst. **73**, 189 (2004), DOI: 10.1016/j.chemolab.2004.03.004.

[68] A. Lorber and B.R. Kowalski, J. Chemom. **2**, 67 (1988), DOI: 10.1002/cem.1180020108.

[69] S. Wold, M. Sjöström, and L. Eriksson, Chemom. Intell. Lab. Syst. **58**, 109 (2001), DOI: 10.1016/S0169-7439(01)00155-1.

[70] S. Wold, Pattern Recogn. **8**, 127 (1976), DOI: 10.1016/0031-3203(76)90014-5.

[71] M.H. Losvik, Plant Ecol. **78**, 157 (1988), DOI: 10.1007/BF00033425.

[72] J.S. Shenk, J.J. Workman, and M.O. Westerhaus, in *Handbook of Near-Infrared Analysis*, 2nd ed., edited by D.A. Burns and E.W. Ciurczak (Marcel Dekker, New York, 2001), p. 419.

[73] M.A. Dearth, Ind. Engl. Chem. Res. **38**, 2203 (1999), DOI: 10.1021/ie980116s.